Wigner $6j$ symbols with gluon lines: completing the set of $6j$ symbols required for color decomposition

Stefan Keppeler [iD],[a] **Simon Plätzer** [iD][b,c,d] **and Malin Sjodahl** [iD][e]

[a]*Fachbereich Mathematik, Universität Tübingen,*
 Auf der Morgenstelle 10, 72076 Tübingen, Germany

[b]*Institute of Physics, NAWI Graz, University of Graz,*
 Universitätsplatz 5, A-8010 Graz, Austria

[c]*Particle Physics, Faculty of Physics, University of Vienna,*
 Boltzmanngasse 5, A-1090 Wien, Austria

[d]*Erwin Schrödinger Institute for Mathematics and Physics, University of Vienna,*
 Boltzmanngasse 9, A-1090 Wien, Austria

[e]*Department of Physics, Lund University,*
 Box 118, 221 00 Lund, Sweden

 E-mail: stefan.keppeler@uni-tuebingen.de, simon.plaetzer@uni-graz.at, malin.sjodahl@fysik.lu.se

ABSTRACT: We construct a set of Wigner $6j$ symbols with gluon lines (adjoint representations) in closed form, expressed in terms of similar $6j$ symbols with quark lines (fundamental representations). Together with these Wigner $6j$ symbols with quark lines, this gives a set of $6j$ symbols sufficient for treating QCD color structure for any number of external particles, in or beyond perturbation theory. This facilitates a complete treatment of QCD color structure in terms of orthogonal multiplet bases, without the need of ever explicitly constructing the corresponding bases. We thereby open up for a completely representation theory based treatment of SU(N) color structure, with the potential of significantly speeding up the color structure treatment.

https://doi.org/10.1007/JHEP05(2024)051

Contents

1 Introduction

A major challenge for accurate predictions of collision rates for processes involving many colored patrons, is the treatment of the $\mathsf{SU}(N)$ color space associated with QCD. This challenge is typically addressed by expanding in color bases, often trace bases [1–12] or color-flow bases [12–19], and sometimes accompanied by sampling of the color states [16, 18–20].

A problem with the trace and color-flow bases is that they are only orthogonal in the limit $N \to \infty$, and in fact overcomplete for many particles; for high multiplicities they are severely overcomplete [21], with a dimension that scales as the factorial of the number of gluons plus quark-antiquark pairs. If one does not want to exploit sampling over different color structures,[1] like done in for example the CVolver program [16, 18, 22], this gives rise to a major bottle neck for the squaring of the color structure, which then scales as a factorial square.

It appears appealing to explore minimal orthogonal bases. This is accomplished by multiplet bases [21, 23–33], which rely on the Clebsch-Gordan decomposition of the involved particle representation for constructing orthogonal bases. Examples of multiplet bases can be found in refs. [23–26], and a general construction in refs. [27, 32, 33].

However, it is possible to do better than that: any color structure can be decomposed into a multiplet basis *without* explicitly constructing this basis, by making use of the group invariant Wigner $6j$ symbols (here $6j$s for short, also known as $6j$ coefficients, Racah coefficients, or Racah W coefficients, up to signs), along with Wigner $3j$ coefficients and dimensions of representations. The problem of decomposing the color structure is then essentially *reduced*

---

[1]Typically the sampling is also accompanied by detailed relations of color flows and kinematic quantities.

to the problem of finding a sufficient set of $6j$ symbols for the color decomposition in question. Some work in this direction has been pursued in refs. [21, 33], where symmetry is exploited to recursively calculate a set of $6j$ symbols applicable for processes with a limited number of partons. Other recent work obtains $\mathsf{SU}(3)$ $6j$ symbols numerically, by first calculating $\mathsf{SU}(3)$ Clebsch-Gordan coefficients [34, 35]. For $\mathsf{SU}(2)$, the problem is addressed in ref. [36].

In a recent paper [37], we started to explore a third avenue, namely to recursively derive $6j$ symbols in terms of other $6j$ symbols and dimensions of representations. We there derived closed forms of a set of $6j$ symbols characterized by having quarks (fundamental representations) in opposing positions. In the present paper, we complete this set of $6j$ symbols with symbols where two of the opposing representations are quarks *or* gluons (adjoint representations), and $6j$s where one vertex only contains fundamental and adjoint representations, whereas the other representations are arbitrary. As we will see, this class of $6j$s defines a complete set for decomposing any color structure appearing in the standard model.

We lay out the basics of $\mathsf{SU}(N)$ color calculations using the birdtrack method in section 2. In section 3 we go through a general procedure for decomposing the color structure. This allows us to identify a set of $6j$ symbols that is sufficient to decompose any color structure to any order in perturbation theory. While one of the necessary classes of $6j$ symbols is calculated in ref. [37], the remaining ones are calculated in section 5, after a careful discussion on how to define vertices in section 4. Finally, we make concluding remarks in section 6.

2 Reducing $\mathsf{SU}(N)$ color structure in birdtrack notation

In this section we briefly outline how to calculate $\mathsf{SU}(N)$ invariants, using the birdtrack method, and assuming knowledge of a sufficient set of Wigner $3j$,[2] and Wigner $6j$ symbols. It is worth remarking that while our discussion focuses on $\mathsf{SU}(N)$, in particular $\mathsf{SU}(3)$, this reduction method is applicable for any Lie group. For a full, comprehensive introduction to the birdtrack formalism, we refer to ref. [38], a minimal introduction can be found in appendix A of ref. [27], whereas a more pedagogical account is written up in ref. [39]. Examples of birdtrack calculations for QCD can be found in refs. [28] and [21].

As we are interested in fully color summed (averaged) color structures, every color structure can be seen as a fully connected graph of $\mathsf{SU}(N)$ representations. While one may treat each color structure coming from each possible Feynman diagram separately, resulting in connected graphs with only (anti)triples and octets, processes with many partons are better handled by having the color structure decomposed into a basis, for example as indicated in figure 1, illustrating a general QCD color structure (including several loops) decomposed into a multiplet basis [21, 27, 32, 33]. This is applicable whether one uses a fixed order perturbative calculation, a full color parton shower or a more sophisticated resummation algorithm. The color basis entails of course triplet and octet representations, but also the higher-dimensional irreducible representations (irreps), used for constructing orthogonal basis vectors. Squaring the color structure is trivial once it has been expanded in an orthogonal basis.

Generally (whether one uses a color basis or not), the squared color structure thus consists of (sums of) fully connected birdtrack graphs with loops of various length. For

---

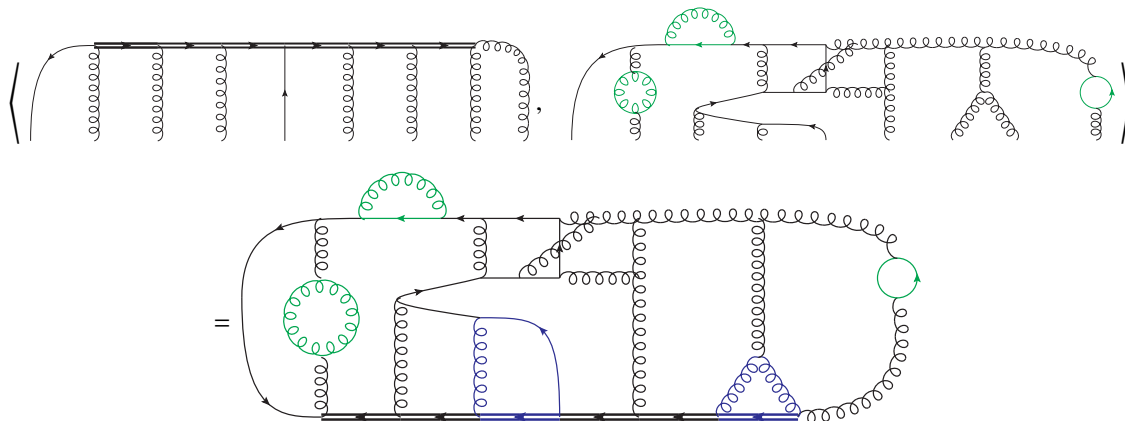[2]We will later normalize the $3j$s to 1.

Figure 1. Example of a scalar product between a basis vector, coming with a set of general representations denoted by double lines, and a general color structure. Note that "bubbles", in green, can be contracted away using eq. (2.9), and that vertex corrections (in blue) can be removed using eq. (2.5). To address the remaining color structure, the completeness relation eq. (2.2) is in general needed.

example, we may encounter

$$,\qquad(2.1)$$

where the double lines denote any irrep of $\mathsf{SU}(N)$, and in general should be supplied with representation labels and arrow directions, which we suppress here for readability.

While short loops of length up to three can be immediately removed (see below), the fall-back method to handle long loops is to split them up to shorter loops by repeated insertion of the completeness relation

$$,\qquad(2.2)$$

where d_δ denotes the dimension of the irrep δ, appearing in the Clebsch-Gordan decomposition, and where the denominator is a Wigner $3j$ symbol.

Tracing both sides of this equation, and using

$$= d_\alpha\,,\qquad(2.3)$$

it is clear that the completeness relation implies $d_\beta d_\gamma = \sum_\delta d_\delta$, as anticipated.

Applying the completeness relation (2.2) to two of the representations in eq. (2.1), marked in red below, schematically results in

$$\tag{2.4}$$

where we now have a "vertex correction" loop with three internal representations. This loop can be removed using the Wigner $6j$ symbols

$$\tag{2.5}$$

Wigner-$6j$

The sum above runs over instances a of the irrep ρ in $\alpha \otimes \sigma$, for example the two octets in $8 \otimes 8 = 1 \oplus 8 \oplus 8 \oplus 10 \oplus \overline{10} \oplus 27$. In this paper, every encountered vertex will contain at least one fundamental or adjoint representation, implying that most often there is only one instance, but for $A \otimes \sigma$, with A being the adjoint representation for $\mathsf{SU}(N)$, and σ being an arbitrary irrep, there can be up to $N - 1$ representations of type σ [27]. We will choose the corresponding vertices to be mutually orthogonal, in the sense that

$$\left\langle \quad , \quad \right\rangle = \qquad \overset{!}{=} 0 \qquad \text{if} \qquad a \neq b. \tag{2.6}$$

Furthermore, for the $6j$ symbols that we derive, we choose to normalize our vertices such that

$$\equiv \delta_{ab}, \quad \text{for all non-vanishing vertices,} \tag{2.7}$$

i.e., the $3j$ coefficients are normalized to one. This implies in particular that $= 1$,

in contrast to the standard QCD normalization $= \frac{1}{2}(N^2 - 1)$, for the generator normalization $\mathrm{tr}[t^a t^b] = \frac{1}{2}\delta^{ab}$. We explain in appendix D how to easily transform our results to any desired normalization.

Note that after having applied eq. (2.5) to eq. (2.4), we are left with a loop with one representation less,

$$
\underset{(2.2)}{=} \sum_\alpha \frac{d_\alpha}{\ominus} \quad \alpha \quad \underset{(2.5)}{=} \sum_\alpha \frac{d_\alpha}{\ominus} \frac{\triangle}{\ominus} \quad \alpha \quad .
$$

(2.8)

Repeatedly applying this procedure to eq. (2.1), it is thus possible to reduce loops with any number of internal representations down to loops of length three (removed using eq. (2.5)) or length two, removed using the "self energy" relation

$$
\overset{\alpha}{\underset{\delta}{\overset{\gamma}{\bigcirc}}}\overset{\beta}{} = \frac{\overset{\gamma}{\underset{\alpha}{\bigoplus}}^{\delta}}{d_\alpha} \quad \overset{\alpha}{=\!=\!=}\overset{\beta}{} \quad .
$$

(2.9)

In this way, assuming the knowledge of the $6j$ symbols, it is possible to reduce any fully connected graph to a number.

It should be noted that the required set of $6j$s depends on how the contraction is performed, and what basis vectors are (possibly) used. In the present paper, we consider basis vectors of the form,

$$
\overset{\alpha_1 \quad \alpha_2 \quad \cdots\cdots \quad \alpha_n}{} \quad ,
$$

(2.10)

where we have a backbone chain of general representations $\alpha_1, \alpha_2, \cdots, \alpha_n$, denoted by double lines with suppressed arrows, to which the external particle representations, octets, triplets and antitriplets, denoted by single lines, are attached (also with suppressed arrows). To the authors' knowledge all multiplet bases in the literature are of this form. One could also imagine bases where general irreps are contracted in vertices. Such bases will require $6j$ symbols beyond those presented here, and are therefore beyond the scope of this paper. We emphasize once more, that the philosophy underlying the present work is to avoid explicitly constructing any bases, and instead achieve a decomposition using $6j$s.

3 A sufficient set of $6j$ symbols for decomposing color structure

In this section we identify a sufficient set of $6j$ symbols for decomposing color structure into the orthogonal basis vectors in eq. (2.10) to any order in perturbation theory. We start out with considering tree-level color structures, and return to higher orders later.
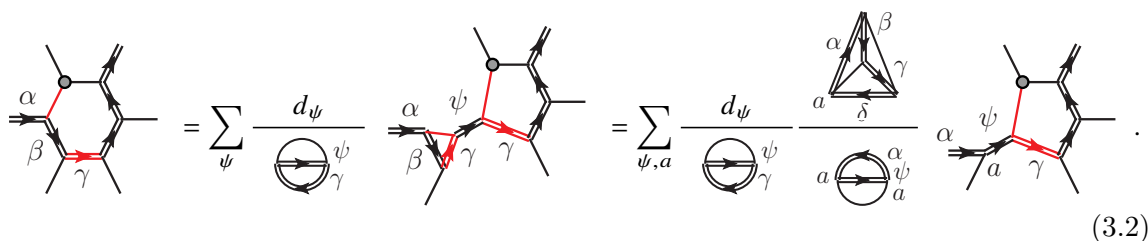
Again, letting single lines schematically denote triplet, octet or singlet representations (i.e. representations of the external particles) and letting double lines denote the general irreps

encountered in the basis vectors, the fully connected graph for a tree-level color structure contracted with a basis vector, will always contain at least two loops of the form
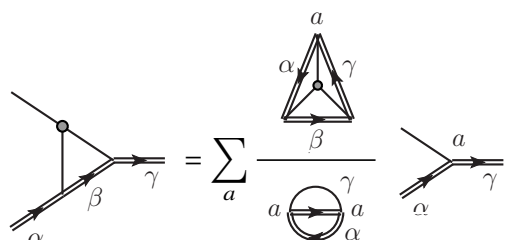
$$\tag{3.1}$$

where the characterizing feature is that there is only one vertex from the initial color structure (the gray blob, representing a quark-gluon or triple-gluon vertex). Typically the color structure will contain many color structures that are trivial to contract using eq. (2.5) and eq. (2.9), but we here consider a worst, general case. To reduce loops of this type, the completeness relation, eq. (2.2), and the vertex correction relation, eq. (2.5), can be applied to the two red representations below

$$\tag{3.2}$$

Repeating this procedure will eventually result in a vertex correction containing the gray blob. (For the loop in the above example, this step would need to be repeated two more times.) The vertex correction with the gray blob gives

$$\tag{3.3}$$

for some representations α, β and γ. This last step removes two vertices, one gray blob, i.e., a vertex from the initial color structure and one vertex between arbitrary representations in the basis vector, eq. (2.10). As every contracted loop removes one vertex from the basis vector and one from the color structure to be decomposed, the resulting graph is topologically equivalent to a graph for a tree-level color structure with one less external patron. After a loop of the form of eq. (3.1) has been contracted, there must thus exist at least two loops of the type in eq. (3.1) in the resulting color structure by the above argument. Hence any tree-level color structure can be completely contracted by repeatedly contracting loops of the form of eq. (3.1).

Only treating loops of the form of eq. (3.1) is thus sufficient for tree-level color structures. We now address the situation where the color structure to be decomposed itself contains loops. It is then not always possible to choose color loops of the form in eq. (2.10). At one-loop

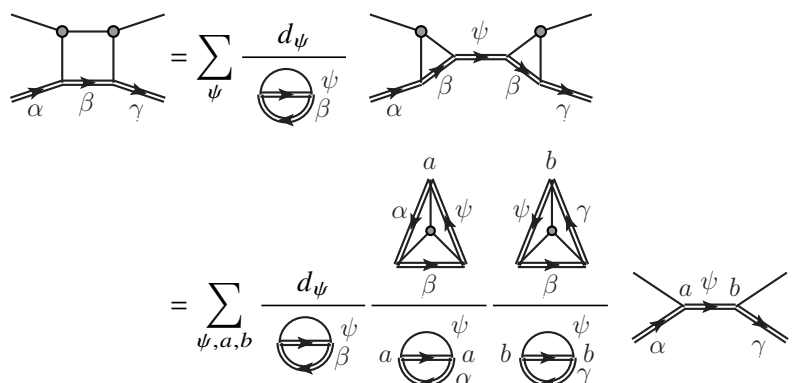this happens for diagrams where all external partons form a single loop

$$\tag{3.4}$$

(For all other one-loop color structures there is at least one vertex with two uncontracted indices, implying that a loop of the from in eq. (3.1) can be found, such that it is possible to contract loops as in eq. (3.2).) For color structures of the form of eq. (3.4), there always exists loops of the form

$$\tag{3.5}$$

Similarly to the loop in eq. (3.1), the steps detailed in eq. (3.2) remain valid. However, at the end, instead of contracting a loop of the form in eq. (3.3), a loop with four vertices is encountered,

$$\tag{3.6}$$

Treating a loop like this removes two vertices from the color structure, and none from the basis vector. Since a one-loop color structure has two vertices more than a tree-level color structure for the same process, the number of vertices after the contraction matches a tree-level structure. Since two legs which initially belonged to the loop of the color structure to be decomposed (the upper legs in eq. (3.6)) now attach directly to the sequence of basis vector representations, the topology after the contraction is equivalent to that of a tree-level color structure. Note that a loop of the type in eq. (3.5), need not be the first loop to be contracted (most one-loop diagrams contain no loop of the form in eq. (3.4)), but such loops may at some point be encountered, and necessary to contract to continue the reduction. In this way, we can thus contract any one-loop diagram. Color structures of arbitrary order in perturbation theory can be decomposed by contracting loops similar to eq. (3.2) and eq. (3.6), possibly with more than two (cf. eq. (3.6)) vertices from the initial color structure. The final steps in the contraction would then proceed as in eq. (3.6), but with more completeness relations inserted.

$n_g = 0$	$n_g = 1$		$n_g = 2$	$n_g = 3$	
case 0	case 1	case 2	case 3	case 4	

Table 1. The required set of $6j$ symbols for color decomposition into multiplet bases of the form in (2.10). The last two $6j$s have the antisymmetric (f) and symmetric (d) triple-gluon vertices in the middle respectively.

In the above color decomposition procedure, we can identify a minimal set of necessary $6j$ symbols, namely those appearing in the different steps above, eqs. (3.2)–(3.3) and eq. (3.6). Keeping in mind that the single lines above denote adjoint or fundamental representations, we conclude that the $6j$s we are after can be divided into the cases in table 1.

We note that the $6j$s of type (0) in table 1 are known from ref. [37]. In this article we address the computation of the remaining $6j$s. Before taking on this task, we must, however, be careful with how we define the vertices for the cases where we have more than one vertex between the same set of representations, which can happen for vertices with gluons, as discussed below eq. (2.5).

4 Vertex construction

In table 1 we sorted the $6j$ symbols that we are going to study in this work according to the number of gluon lines and according to the number of vertices with gluon lines that these $6j$ symbols contain. Before we can evaluate the $6j$ symbols, we have to construct all vertices with at least one gluon line. When discussing how many vertices with a given set of irreps there are, it is useful to think of the general irrep labels (for which we use Greek letters) as Young diagrams. In fact, a systematic labeling of $\mathsf{SU}(N)$ irreps applicable for *arbitrary N* should rather be in terms of pairs of Young diagrams [33, 40]. However, if we allow for Young diagrams with columns with an N-dependent number of boxes, we can replace each pair of Young diagrams by a single Young diagram [33]. For instance, the adjoint representation is then labeled by the Young diagram $A = \blacksquare$, where, here and in what follows, a black column always represents a column with $N-1$ boxes. Hence, in the following, we can always think of irrep labels as single Young diagrams with, possibly, N-dependent column lengths.

We will normalize all our vertices such that all non-vanishing $3j$ symbols are equal to 1, as already mentioned following eq. (2.6). Readers who prefer to work with different normalizations are referred to appendix D for a simple transformation rule.

For each instance of the irrep α in the complete reduction of $\gamma \otimes A$ we have to construct a vertex

$$\tag{4.1}$$

where a thus runs from 1 to the multiplicity of α in $\gamma \otimes A$. Essentially, we construct these vertices by splitting the gluon line into a $q\bar{q}$-pair. More precisely, we consider all diagrams

$$(4.2)$$

where j enumerates admissible intermediate irreps according to a scheme to be explained below, and construct the desired vertices as linear combinations of these diagrams. In general, these vertices then take the form

$$(4.3)$$

with coefficients $C_{aj}^{\alpha\gamma} \in \mathbb{C}$, which will actually turn out to be real-valued functions of N. We distinguish the two cases $\alpha \neq \gamma$ and $\alpha = \gamma$.

If $\alpha \neq \gamma$ then there is only a non-zero vertex (4.1) if α can be found in the Clebsch-Gordan decomposition of $\gamma \otimes A$. This means that we can obtain α from γ by adding a box in one row and subsequently removing a box in a different row (possibly after first adding a column of length N) [27]. In this case there is a unique intermediate irrep λ_1 in diagram (4.2), representing the intermediate step in this process after adding a box but before removing the other box. Hence, for such $\alpha \neq \gamma$, we find

$$(4.4)$$

where the constant has to be chosen such that the normalization condition for the corresponding $3j$ symbol,

$$(4.5)$$

is fulfilled. After a few steps, spelled out in appendix A, we get from eq. (A.8)

$$C_{11}^{\alpha\gamma} = \sqrt{d_{\lambda_1}(N^2 - 1)} \quad \text{for} \quad \alpha \neq \gamma \,. \tag{4.6}$$

For $\alpha = \gamma$ there can be up to $N-1$ vertices of type (4.1), cf. appendix B of ref. [27], i.e., if the multiplicity of α in the complete reduction of $\alpha \otimes A$ is K, we have to construct the vertices

$$a = 1, \ldots, K \,. \tag{4.7}$$

In this case there exist $K + 1$ different admissible irreps λ_j rendering the diagrams

$$
\vcenter{\hbox{}} \quad , \quad j = 1, \ldots, K + 1 \,, \tag{4.8}
$$

non-zero, as discussed in appendix A, where we also show that all vertices in eq. (4.7) are linear combinations of theses diagrams, i.e.

$$
\vcenter{\hbox{}} = \sum_j C_{aj}^{\alpha\alpha} \vcenter{\hbox{}} \,. \tag{4.9}
$$

Hence, we can obtain a set of orthonormal vertices (4.7) by applying the Gram-Schmidt algorithm to the set of diagrams (4.8) with admissible intermediate irreps λ_j.

In order to obtain a unique result when carrying out Gram-Schmidt we have to decide how to sort the diagrams (4.8). To this end, note that an admissible λ_j is obtained by adding an extra box to α. We say that

$$
\vcenter{\hbox{}} < \vcenter{\hbox{}} \tag{4.10}
$$

if in λ_k this extra box is added further down compared to where it was added in λ_j. We then sort the birdtrack diagrams (4.8) in increasing order. Hence, the first birdtrack diagram in our list is always the diagram with intermediate irrep λ_1 which is obtained by adding a box to the first row of α. In appendix A we show that the last diagram in this list is always a linear combinations of the first K diagrams and can thus be omitted. The sum in eq. (4.9) hence runs from 1 to K.

In order to carry out Gram-Schmidt we only need to know the scalar products between all diagrams (4.8), which are calculated in appendix A, eq. (A.6)–(A.8). We denote this

$$
s_{jk} = \left\langle \vcenter{\hbox{}} \,, \vcenter{\hbox{}} \right\rangle = \frac{1}{N^2 - 1} \left(\frac{\delta_{jk}}{d_{\lambda_j}} - \frac{1}{N d_\alpha} \right) \,. \tag{4.11}
$$

The scalar products s_{jk} also depend on the irrep α but we do not display this dependence in our notation since in the following s_{jk} for different irreps α never appear alongside each other in our equations.

We explicitly state the formulae for the first two vertices, which are the only vertices in the physically relevant case $N = 3$,

$$
\vcenter{\hbox{}} = \frac{1}{\sqrt{s_{11}}} \vcenter{\hbox{}} \tag{4.12}
$$

$$\text{(diagram)} = \sqrt{\frac{s_{11}}{s_{11}s_{22} - s_{12}^2}} \left(\text{(diagram)} - \frac{s_{12}}{s_{11}} \text{(diagram)} \right) \qquad (4.13)$$

Further vertices, which only exist for $N > 3$, are calculated by straightforwardly continuing Gram-Schmidt. In appendix B we illustrate the explicit vertex construction with a few examples.

5 Formulae for gluon $6j$ symbols

We will now describe how the calculation of the different classes of $6j$ symbols proceeds. Our main tool will be the repeated insertion of vertex corrections, and the Fierz identity, eq. (A.7), to decompose gluon lines. We will go through the basic idea and steps for the simpler cases here, but defer the details of longer calculations to appendix C for the sake of readability.

Case 1: $6j$s with a quark-gluon vertex. We here consider the $6j$ symbol which contains a $q\bar{q}g$ vertex (in its center). We proceed to calculate this by expanding the gluon vertex into a vertex correction

$$\text{(diagram)} \xrightarrow{(4.4)} \sqrt{d_{\lambda_1}(N^2 - 1)} \; \text{(diagram)} \xrightarrow{(A.8)} \frac{\delta_{\beta\lambda_1}}{\sqrt{d_\beta(N^2 - 1)}}, \qquad (5.1)$$

where we have assumed $\alpha \neq \gamma$ and used eq. (A.8) from appendix A, which builds on the Fierz identity, eq. (A.7).

In the case $\alpha = \gamma$, again using eq. (A.8), for the first two vertices $a = 1, 2$ we obtain

$$\text{(diagram)} \xrightarrow{(4.12)} \frac{s_{1k}}{\sqrt{s_{11}}} \qquad \text{and} \qquad (5.2)$$

$$\text{(diagram)} \xrightarrow{(4.13)} \sqrt{\frac{s_{11}}{s_{11}s_{22} - s_{12}^2}} \left(s_{2k} - \frac{s_{12}}{s_{11}} s_{1k} \right). \qquad (5.3)$$

Note that the last expression vanishes for $k = 1$. For $N > 3$, there might, as described, be more vertices which then are treated similarly.

Case 2: 6js with a gluon line opposing a quark line. In this case we have one quark and one gluon line attaching to different vertices. Rewriting the gluon vertices in terms of vertex corrections and invoking the Fierz identity, we then find, after a few steps spelled out in appendix C,

$$
\begin{array}{c}
\text{(diagram)}
\end{array}
= \sum_{j=1}^{a} \sum_{k=1}^{b} \frac{C_{aj}^{\beta\alpha} C_{bk}^{\delta\gamma}}{N^2-1} \left(\text{(diagram)} \quad \text{(diagram)} - \frac{\delta_{\alpha\beta}\, \delta_{\gamma\delta}}{N d_\alpha\, d_\gamma} \right), \quad (5.4)
$$

where the 6j symbols with two quark lines are given in closed form in ref. [37].

Case 3: 6js with two opposing gluon lines. Case 3 can be addressed with a similar strategy as the other cases. Our result, for which we demonstrate all intermediate steps in appendix C, reads

$$
\begin{array}{c}
\text{(diagram)}
\end{array}
= \sum_{j=1}^{a} \sum_{k=1}^{b} \frac{C_{aj}^{\beta\alpha} C_{bk}^{\delta\gamma}}{N^2-1} \left(\text{(diagram)} \quad \text{(diagram)} - \frac{\delta_{\alpha\beta}\, \delta_{\gamma\delta}}{N d_\alpha\, d_\gamma} \right). \quad (5.5)
$$

Case 4: 6js with three-gluon vertices. For the class of 6j symbols with triple-gluon vertices, we distinguish the case in which the triple-gluon vertex is proportional to if^{abc} from the case in which it is proportional to d^{abc}. We will illustrate the case of if^{abc} first. In particular, we use the definition of the if^{abc}-vertex in terms of traces, and then insert vertex corrections,

$$
\begin{array}{c}
\text{(diagram)}
\end{array}
= \frac{N^2-1}{\sqrt{2N}} \left(\text{(diagram)} - \text{(diagram)} \right). \quad (5.6)
$$

Using the Fierz identity, eq. (A.7), we can remove all internal gluon lines and the results are expressed in terms of a number of different diagrams which reduce to 3j symbols, dimensions and traces over quark lines, see appendix C. A single non-trivial diagram remains, which can be expressed as

$$
\begin{array}{c}
\text{(diagram)}
\end{array}
= \sum_{\sigma} d_\sigma \left(\text{(diagram)} - \text{(diagram)} - \text{(diagram)} \right), \quad (5.7)
$$

where a minus sign next to a vertex indicates that the lines are connected to this vertex in opposite order, i.e.

$$
\begin{array}{c}
\includegraphics{eq58a}
\end{array}
=
\begin{array}{c}
\includegraphics{eq58b}
\end{array}, \tag{5.8}
$$

see also appendix C of ref. [37]. For the above vertices with quarks this only makes a difference for the antisymmetic vertex of $q \otimes q$ see ref. [37] Our final result for the f-vertex is

$$
= \frac{1}{(N^2-1)^2} \frac{1}{\sqrt{2N}} \sum_{j=1}^{a} \sum_{k=1}^{b} \sum_{\ell=1}^{c} C_{aj}^{\beta\alpha} C_{bk}^{\gamma\beta} C_{c\ell}^{\alpha\gamma}
$$

$$
\left(\sum_{\sigma} d_{\sigma} \quad
\begin{array}{c}\includegraphics{t1}\end{array}
\begin{array}{c}\includegraphics{t2}\end{array}
\begin{array}{c}\includegraphics{t3}\end{array}
- \frac{\delta_{\lambda_j \mu_k} \, \delta_{\lambda_j \nu_\ell}}{d_{\lambda_j}^2} \right), \tag{5.9}
$$

while we obtain for the d-vertex,

$$
= \frac{1}{(N^2-1)^2} \sqrt{\frac{N}{2(N^2-4)}} \sum_{j=1}^{a} \sum_{k=1}^{b} \sum_{\ell=1}^{c} C_{aj}^{\beta\alpha} C_{bk}^{\gamma\beta} C_{c\ell}^{\alpha\gamma}
$$

$$
\left(\sum_{\sigma} d_{\sigma} \quad
\begin{array}{c}\includegraphics{t1}\end{array}
\begin{array}{c}\includegraphics{t2}\end{array}
\begin{array}{c}\includegraphics{t3}\end{array}
+ \frac{\delta_{\lambda_j \mu_k} \, \delta_{\lambda_j \nu_\ell}}{d_{\lambda_j}^2} \right.
$$

$$
\left. + \frac{4}{N^2} \frac{\delta_{\alpha\beta} \, \delta_{\alpha\gamma}}{d_\alpha^2} - \frac{2}{N} \left(\frac{\delta_{\alpha\gamma} \, \delta_{\lambda_j \mu_k}}{d_\alpha \, d_{\lambda_j}} + \frac{\delta_{\alpha\beta} \, \delta_{\mu_k \nu_\ell}}{d_\alpha \, d_{\mu_k}} + \frac{\delta_{\beta\gamma} \, \delta_{\lambda_j \nu_\ell}}{d_\beta \, d_{\lambda_j}} \right) \right). \tag{5.10}
$$

6 Conclusions and outlook

In the present paper we have shown how to calculate a set of Wigner $6j$ coefficients with adjoint representations. Together with a set of previously derived $6j$s [37], this set constitutes

a complete set of $6j$s required to decompose any color structure, to any order into orthogonal multiplet bases, cf. eq. (2.10).

This opens up for the usage of orthogonal representation theory based color bases also for processes with high multiplicities, including the analysis of evolution equations in color space [41].

We note, however, that the present work does not close the research area of representation theory based treatment of color structure. In particular, more general $6j$ symbols are required for fully general multiplet bases (with vertices between general representations). We believe that this can be addressed with similar methods.

Acknowledgments

A   Properties of vertex correction diagrams

We discuss some properties of the vertex correction diagrams in eq. (4.2), which we use for the construction of vertices with at least one gluon. Let K be the multiplicity of α in the complete reduction of $\alpha \otimes A$, giving the number of vertices (4.7) to be constructed. In contrast, the number of intermediate irreps λ_j in eq. (4.8) is given by the multiplicity of α in the complete reduction of $\alpha \otimes \square \otimes \overline{\square}$. The latter number is one higher than the former since due to $\square \otimes \overline{\square} = A \otimes \bullet$ (where $\bullet$ denotes the trivial representation) we have $\alpha \otimes \square \otimes \overline{\square} = (\alpha \otimes A) \oplus \alpha$. Moreover, $K + 1$ is also the number of terms in the complete reduction of $\alpha \otimes \square$, i.e. the number of ways in which we can add a box to the Young diagram α.

First we show that the diagrams in eq. (4.8) are linearly dependent. To this end, consider the complete reduction of $\alpha \otimes \square$,

$$\tag{A.1}$$

multiply with a quark-gluon vertex (Lie algebra generators), and contract the quark and antiquark lines, yielding

$$\tag{A.2}$$

The l.h.s. vanishes since the $\mathsf{SU}(N)$ generators are traceless, i.e. we have found a non-trivial vanishing linear combination of the diagrams in eq. (4.8).

Next we show that all vertices in eq. (4.7) are linear combinations of the diagrams in eq. (4.8). To this end, consider a gluon exchange between α and a quark line, and insert two completeness relations:

$$
\begin{array}{c} \text{(diagram)} \end{array} = \sum_{j,k=1}^{K+1} d_{\lambda_j}\, d_{\lambda_k} \begin{array}{c} \text{(diagram)} \end{array}. \tag{A.3}
$$

Due to Schur's Lemma the middle segment can only be non-zero if λ_j and λ_k are equivalent. If two irreps in the complete reduction of $\alpha \otimes \square$ are equivalent then they are the same, i.e.

$$
\begin{array}{c} \text{(diagram)} \end{array} = \widetilde{C}_{aj}\, \delta_{jk} \begin{array}{c} \text{(diagram)} \end{array} \tag{A.4}
$$

with some constant $\widetilde{C}_{aj}$. Substituting into eq. (A.3), multiplying with a quark-gluon vertex, and contracting the quark and antiquark line we find

$$
\begin{array}{c} \text{(diagram)} \end{array} = \sum_{j=1}^{K+1} \widetilde{C}_{aj}\, d_{\lambda_j}^2 \begin{array}{c} \text{(diagram)} \end{array}. \tag{A.5}
$$

The quark loop on the l.h.s. can be traded for a factor of $(N^2 - 1)^{-1}$ (recall that we set all $3j$ symbols equal to 1), and by defining $C_{aj}^{\alpha\alpha} = \widetilde{C}_{aj}\, d_{\lambda_j}^2\, (N^2 - 1)$ we obtain eq. (4.9), as claimed in section 4.

Now we can even take advantage of the linear dependence (A.2) of the vertex correction diagrams (4.8). Equation (A.2) tells us that any one of the $K+1$ diagrams (4.8) can be expressed as a linear combination of the other K diagrams, since none of the coefficients in eq. (A.2) vanishes. In section 4 we order the diagrams in a unique way and determine the orthonormal vertices in eq. (4.7) by means of the Gram-Schmidt algorithm. Since the last vertex correction diagram is guaranteed to be a linear combination of the first K diagrams, we can always terminate Gram-Schmidt *before* using the last diagram, i.e the vertices (4.7) are actually linear combinations of the first K vertex correction diagrams (4.8).

Finally, we explicitly determine the scalar products between all vertex correction diagrams (4.2). The result is the main ingredient for the Gram-Schmidt process in section 4. Consider

$$
\left\langle \begin{array}{c} \text{(diagram)} \end{array}, \begin{array}{c} \text{(diagram)} \end{array} \right\rangle = \begin{array}{c} \text{(diagram)} \end{array}. \tag{A.6}
$$

The square diagram can be evaluated by invoking the Fierz identity (or adjoint representation projector, also equivalent to the completeness relation for $q \otimes \bar{q}$), which with our unit $3j$

symbols takes the form

$$\text{(A.7)} \qquad = \frac{1}{N^2-1}\left(\quad - \frac{1}{N} \quad \right).$$

Inserting this gives for the scalar product

$$
= \frac{1}{N^2-1}\left(\quad - \frac{1}{N} \quad \right)
$$

(A.8)

$$
= \frac{1}{N^2-1}\left(\frac{\delta_{\beta\delta}}{d_\beta} - \frac{\delta_{\alpha\gamma}}{N d_\alpha} \right).
$$

B Examples of vertex construction

We illustrate how to construct vertices of type (4.1) using methods and results from section 4.

First consider an example with $\alpha \neq \gamma$. For $\alpha = \Box$ and $\gamma = \Box\Box$ the unique intermediate irrep is $\lambda_1 = \Box\Box$. Then, using eq. (4.6) for normalization, the unique vertex with irreps $\Box$, $\Box\Box$ and one gluon reads

$$
= (N^2-1)\sqrt{\frac{N}{3}} \qquad . \tag{B.1}
$$

The Young diagram with the smallest number of boxes for which there is more than one vertex is $\alpha = \gamma = \Box\Box$, i.e., the octet for $N = 3$ (note that this is *not* the adjoint representation for $N \neq 3$). The admissible intermediate irreps are $\lambda_1 = \Box\Box\Box$ and $\lambda_2 = \Box\Box$. Using eq. (4.13), the orthonormal vertices become

$$
= N(N^2-1)\sqrt{\frac{N+2}{5N-6}} \qquad \text{and} \tag{B.2}
$$

$$
= \frac{N(N^2-1)}{6}\sqrt{\frac{5N-6}{N-2}}\left(\quad + 3\frac{N+2}{5N-6} \quad \right). \tag{B.3}
$$

For $\alpha = \gamma = A = \blacksquare\Box$ (recall that the black column stands for a column with $N-1$ boxes) we obtain three-gluon vertices for general N. The admissible intermediate irreps are then

$\lambda_1 = \blacksquare\square\square$ and $\lambda_2 = \blacksquare\square$. Using eq. (4.13), our orthonormal vertices read

$$\text{(diagram 1)} = (N^2 - 1)\sqrt{N+2}\ \ \text{(diagram)} \qquad \text{and} \tag{B.4}$$

$$\text{(diagram 2)} = \frac{N(N^2-1)}{2}\sqrt{N-2}\left(\text{(diagram)} + \frac{N+2}{N}\ \text{(diagram)} \right). \tag{B.5}$$

Notice that for $N = 3$ eqs. (B.2)/(B.3) and eqs. (B.4)/(B.5) coincide. Instead of the latter vertices, one will likely want to use the much more common antisymmetric f and symmetric d vertices, to which our vertices are related by a unitary transformation, which we explicitly state below. Like all other vertices in this article we normalize f and d such that the corresponding $3j$ symbols are equal to one, i.e.

$$\text{(diagram)} = \frac{N^2-1}{\sqrt{2N}}\left(\text{(diagram)} - \text{(diagram)} \right) \qquad \text{and} \tag{B.6}$$

$$\text{(diagram)} = (N^2-1)\sqrt{\frac{N}{2(N^2-4)}}\left(\text{(diagram)} + \text{(diagram)} \right), \tag{B.7}$$

see appendix D for how to easily transform results to other normalizations. The vertices (B.4) and (B.5) are related to f and d by a unitary transformation,

$$\text{(diagram 1)} = -\sqrt{\frac{N+2}{2N}}\ \text{(diagram)} + \sqrt{\frac{N-2}{2N}}\ \text{(diagram)}, \tag{B.8}$$

$$\text{(diagram 2)} = -\sqrt{\frac{N-2}{2N}}\ \text{(diagram)} - \sqrt{\frac{N+2}{2N}}\ \text{(diagram)}, \tag{B.9}$$

and vice versa,

$$\text{(diagram)} = -\sqrt{\frac{N+2}{2N}}\ \text{(diagram 1)} - \sqrt{\frac{N-2}{2N}}\ \text{(diagram 2)}, \tag{B.10}$$

$$\text{(diagram)} = \sqrt{\frac{N-2}{2N}}\ \text{(diagram 1)} - \sqrt{\frac{N+2}{2N}}\ \text{(diagram 2)}, \tag{B.11}$$

facilitating easy conversion.

The coefficients of this unitary transformation are determined by scalar products between the two sets of vertices, and these scalar products can be evaluated by calculations similar to eqs. (A.6)–(A.8).

C Details of $6j$ derivations

We here give, in full detail, the intermediate steps for the derivation in section 5.

Derivation for case 2. We here derive the form of the $6j$ coefficients in eq. (5.4). In essence the vertices involving gluons are expressed in terms of vertex corrections, after which the Fierz identity, eq. (A.7), is applied, and vertex corrections are removed using eq. (2.5)

$$\tag{C.1}$$

Derivation for case 3. The steps in the derivation of eq. (5.5) progress similarly to those in the derivation of eq. (5.4),

$$= \sum_{j=1}^{a}\sum_{k=1}^{b}\frac{C_{aj}^{\beta\alpha}C_{bk}^{\delta\gamma}}{N^2-1}\left(\quad -\frac{1}{N}\quad\right)$$

$$= \sum_{j=1}^{a}\sum_{k=1}^{b}\frac{C_{aj}^{\beta\alpha}C_{bk}^{\delta\gamma}}{N^2-1}\left(\quad -\frac{\delta_{\alpha\beta}\delta_{\gamma\delta}}{Nd_\alpha d_\gamma}\right)$$

$$= \sum_{j=1}^{a}\sum_{k=1}^{b}\frac{C_{aj}^{\beta\alpha}C_{bk}^{\delta\gamma}}{N^2-1}\left(\quad -\frac{\delta_{\alpha\beta}\delta_{\gamma\delta}}{Nd_\alpha d_\gamma}\right). \tag{C.2}$$

We remark that the result looks very similar to the result for case 2, but that it is now expressed in terms of the $6js$ from case 2.

Derivation for case 4. Again the gluon vertices are expressed in terms of vertex corrections with quarks, both in the triple-gluon vertices and in the vertices with the general representations. This gives for the antisymmetric (f) triple-gluon vertex

$$= \frac{N^2-1}{\sqrt{2N}}\left(\quad - \quad\right) \tag{C.3}$$

$$= \frac{N^2-1}{\sqrt{2N}}\sum_{j=1}^{a}\sum_{k=1}^{b}\sum_{\ell=1}^{c}C_{aj}^{\beta\alpha}C_{bk}^{\gamma\beta}C_{c\ell}^{\alpha\gamma}\left(\quad - \quad\right)$$

and the symmetric (d) vertex differs only by the sign of the second term.

The second term above is calculated using the Fierz identity (A.7),

$$
\frac{1}{(N^2-1)^3} \left[\quad - \frac{1}{N} \left(\quad + \quad + \quad \right) + \frac{3}{N^2} \quad - \frac{1}{N^3} \quad \right], \tag{C.4}
$$

where the closed quark loop in the last diagram simply yields a factor of N, and the others are easy to evaluate using the self energy relation, eq. (2.9), for example

$$
= \frac{\delta_{\lambda_j \mu_k} \, \delta_{\lambda_j \nu_\ell}}{d_{\lambda_j}^2} \,. \tag{C.5}
$$

By identical steps, the first term in eq. (C.3) gives

$$
\frac{1}{(N^2-1)^3} \left[\quad - \frac{1}{N} \left(\quad + \quad + \quad \right) + \frac{3}{N^2} \quad - \frac{1}{N^3} \quad \right]. \tag{C.6}
$$

Here the first term needs to be reduced using $6j$ symbols,

$$\tag{C.7}$$

where a minus sign next to a vertex indicates that the lines are connected to this vertex in opposite order, see eq. (5.8). The expressions calculated here are assembled in eq. (5.9) and eq. (5.10) for the antisymmetric and symmetric vertices, respectively.

D Vertex normalizations leading to non-trivial $3j$ symbols

All explicit formulae for Wigner $6j$ symbols in this article, in particular the results in section 5, are valid for vertices normalized such that all non-vanishing $3j$ symbols are equal to 1. While this normalization is convenient, it differs from normalizations typically applied in the context of QCD. We therefore here give a simple rule for how to transform any of our $6j$ symbols when changing the normalization of any $3j$ symbol.

Assume we have calculated the $6j$ symbol

$$\tag{D.1}$$

whereby we chose the normalization

$= 1\,.$

$$\tag{D.2}$$

If we prefer this $3j$ symbol to be equal to $C \neq 1$ we define a vertex

$$\begin{array}{c}\beta\quad\alpha\\ \gamma\end{array} = \sqrt{C}\ \begin{array}{c}\beta\quad\alpha\\ \gamma\end{array} \quad , \tag{D.3}$$

which then satisfies

$$\begin{array}{c}\alpha\\ \gamma\ \beta\end{array} = C\ \begin{array}{c}\alpha\\ \gamma\ \beta\end{array} = C\ . \tag{D.4}$$

Consequently,

$$\alpha\quad\begin{array}{c}\\ \gamma\\ \beta\end{array} = \sqrt{C}\ \ \alpha\quad\begin{array}{c}\\ \gamma\\ \beta\end{array} \quad . \tag{D.5}$$

In short: for each vertex whose $3j$ symbol you normalize to a number $\neq 1$ multiply our $6j$ symbol by the square root of the value of your $3j$ symbol in order to obtain the value of the $6j$ symbol with your normalization convention.

References

[1] J.E. Paton and H.-M. Chan, *Generalized veneziano model with isospin*, *[Nucl. Phys. B](#)* **10** (1969) 516 [[InSPIRE](#)].

[2] F.A. Berends and W. Giele, *The Six Gluon Process as an Example of Weyl-Van Der Waerden Spinor Calculus*, *[Nucl. Phys. B](#)* **294** (1987) 700 [[InSPIRE](#)].

[3] M.L. Mangano, S.J. Parke and Z. Xu, *Duality and Multi-Gluon Scattering*, *[Nucl. Phys. B](#)* **298** (1988) 653 [[InSPIRE](#)].

[4] M.L. Mangano, *The Color Structure of Gluon Emission*, *[Nucl. Phys. B](#)* **309** (1988) 461 [[InSPIRE](#)].

[5] D.A. Kosower, *Color Factorization for Fermionic Amplitudes*, *[Nucl. Phys. B](#)* **315** (1989) 391 [[InSPIRE](#)].

[6] Z. Nagy and D.E. Soper, *Parton showers with quantum interference*, *[JHEP](#)* **09** (2007) 114 [[arXiv:0706.0017](#)] [[InSPIRE](#)].

[7] M. Sjödahl, *Color structure for soft gluon resummation: A General recipe*, *[JHEP](#)* **09** (2009) 087 [[arXiv:0906.1121](#)] [[InSPIRE](#)].

[8] J. Alwall et al., *MadGraph 5: Going Beyond*, *[JHEP](#)* **06** (2011) 128 [[arXiv:1106.0522](#)] [[InSPIRE](#)].

[9] M. Sjödahl, *ColorFull — a C++ library for calculations in* SU(N_c) *color space*, *Eur. Phys. J. C* **75** (2015) 236 [`arXiv:1412.3967`] [InSPIRE].

[10] S. Plätzer and M. Sjödahl, *Subleading N_c improved Parton Showers*, *JHEP* **07** (2012) 042 [`arXiv:1201.0260`] [InSPIRE].

[11] S. Plätzer, M. Sjödahl and J. Thorén, *Color matrix element corrections for parton showers*, *JHEP* **11** (2018) 009 [`arXiv:1808.00332`] [InSPIRE].

[12] R. Frederix and T. Vitos, *The colour matrix at next-to-leading-colour accuracy for tree-level multi-parton processes*, *JHEP* **12** (2021) 157 [`arXiv:2109.10377`] [InSPIRE].

[13] G. 't Hooft, *A Planar Diagram Theory for Strong Interactions*, *Nucl. Phys. B* **72** (1974) 461 [InSPIRE].

[14] A. Kanaki and C.G. Papadopoulos, *HELAC-PHEGAS: Automatic computation of helicity amplitudes and cross-sections*, *AIP Conf. Proc.* **583** (2002) 169 [`hep-ph/0012004`] [InSPIRE].

[15] F. Maltoni, K. Paul, T. Stelzer and S. Willenbrock, *Color Flow Decomposition of QCD Amplitudes*, *Phys. Rev. D* **67** (2003) 014026 [`hep-ph/0209271`] [InSPIRE].

[16] S. Plätzer, *Summing Large-N Towers in Colour Flow Evolution*, *Eur. Phys. J. C* **74** (2014) 2907 [`arXiv:1312.2448`] [InSPIRE].

[17] R. Ángeles Martínez et al., *Soft gluon evolution and non-global logarithms*, *JHEP* **05** (2018) 044 [`arXiv:1802.08531`] [InSPIRE].

[18] M. De Angelis, J.R. Forshaw and S. Plätzer, *Resummation and Simulation of Soft Gluon Effects beyond Leading Color*, *Phys. Rev. Lett.* **126** (2021) 112001 [`arXiv:2007.09648`] [InSPIRE].

[19] S. Plätzer and I. Ruffa, *Towards Colour Flow Evolution at Two Loops*, *JHEP* **06** (2021) 007 [`arXiv:2012.15215`] [InSPIRE].

[20] J. Isaacson and S. Prestel, *Stochastically sampling color configurations*, *Phys. Rev. D* **99** (2019) 014021 [`arXiv:1806.10102`] [InSPIRE].

[21] M. Sjödahl and J. Thorén, *Decomposing color structure into multiplet bases*, *JHEP* **09** (2015) 055 [`arXiv:1507.03814`] [InSPIRE].

[22] J.R. Forshaw, J. Holguin and S. Plätzer, *Rings and strings: a basis for understanding subleading colour and QCD coherence beyond the two-jet limit*, *JHEP* **05** (2022) 190 [`arXiv:2112.13124`] [InSPIRE].

[23] A. Kyrieleis and M.H. Seymour, *The colour evolution of the process $q\,q \to q\,q\,g$*, *JHEP* **01** (2006) 085 [`hep-ph/0510089`] [InSPIRE].

[24] Y.L. Dokshitzer and G. Marchesini, *Soft gluons at large angles in hadron collisions*, *JHEP* **01** (2006) 007 [`hep-ph/0509078`] [InSPIRE].

[25] M. Sjödahl, *Color evolution of $2 \to 3$ processes*, *JHEP* **12** (2008) 083 [`arXiv:0807.0555`] [InSPIRE].

[26] M. Beneke, P. Falgari and C. Schwinn, *Soft radiation in heavy-particle pair production: All-order colour structure and two-loop anomalous dimension*, *Nucl. Phys. B* **828** (2010) 69 [`arXiv:0907.1443`] [InSPIRE].

[27] S. Keppeler and M. Sjödahl, *Orthogonal multiplet bases in* SU(N_c) *color space*, *JHEP* **09** (2012) 124 [`arXiv:1207.0609`] [InSPIRE].

[28] Y.-J. Du, M. Sjödahl and J. Thorén, *Recursion in multiplet bases for tree-level MHV gluon amplitudes*, *JHEP* **05** (2015) 119 [`arXiv:1503.00530`] [InSPIRE].

[29] S. Keppeler and M. Sjödahl, *Hermitian Young Operators*, *J. Math. Phys.* **55** (2014) 021702 [`arXiv:1307.6147`] [InSPIRE].

[30] J. Alcock-Zeilinger and H. Weigert, *Simplification Rules for Birdtrack Operators*, *J. Math. Phys.* **58** (2017) 051701 [`arXiv:1610.08801`] [InSPIRE].

[31] J. Alcock-Zeilinger and H. Weigert, *Compact Hermitian Young Projection Operators*, *J. Math. Phys.* **58** (2017) 051702 [`arXiv:1610.10088`] [InSPIRE].

[32] J. Alcock-Zeilinger and H. Weigert, *Transition Operators*, *J. Math. Phys.* **58** (2017) 051703 [`arXiv:1610.08802`] [InSPIRE].

[33] M. Sjödahl and J. Thorén, *QCD multiplet bases with arbitrary parton ordering*, *JHEP* **11** (2018) 198 [`arXiv:1809.05002`] [InSPIRE].

[34] A. Alex, M. Kalus, A. Huckleberry and J. von Delft, *A numerical algorithm for the explicit calculation of* SU(N) *and* SL(N, C) *Clebsch-Gordan coefficients*, *J. Math. Phys.* **52** (2011) 023507 [`arXiv:1009.0437`] [InSPIRE].

[35] T. Dytrych et al., *SU3lib: A C++ library for accurate computation of Wigner and Racah coefficients of* SU(3), *Comput. Phys. Commun.* **269** (2021) 108137 [InSPIRE].

[36] H.T. Johansson and C. Forssén, *Fast and Accurate Evaluation of Wigner 3j, 6j, and 9j Symbols Using Prime Factorization and Multiword Integer Arithmetic*, *SIAM J. Sci. Comput.* **38** (2016) A376 [`arXiv:1504.08329`] [InSPIRE].

[37] J. Alcock-Zeilinger, S. Keppeler, S. Plätzer and M. Sjödahl, *Wigner 6j symbols for SU(N): Symbols with at least two quark-lines*, *J. Math. Phys.* **64** (2023) 023504 [`arXiv:2209.15013`] [InSPIRE].

[38] P. Cvitanović, *Group Theory: Birdtracks, Lie's, and Exceptional Groups*, Princeton University Press (2020) [InSPIRE].

[39] S. Keppeler, *Birdtracks for* SU(N), *SciPost Phys. Lect. Notes* **3** (2018) 1 [`arXiv:1707.07280`] [InSPIRE].

[40] R.C. King, *Generalized Young Tableaux and the General Linear Group*, *J. Math. Phys.* **11** (1970) 280.

[41] S. Plätzer, *Colour evolution and infrared physics*, *JHEP* **07** (2023) 126 [`arXiv:2204.06956`] [InSPIRE].